

Synthesis, Characterization, and Adsorption Capacity of Crosslinked Starch Microspheres with *N,N'*-Methylene Bisacrylamide

Xin-Fa Zhao,¹ Zhong-Jin Li,^{1,2} Lei Wang,² Xiao-Juan Lai²

¹School of Resource and Environment, Shaanxi University of Science & Technology, Xi'an 710021, People's Republic of China

²School of Chemistry and Chemical Engineering, Shaanxi University of Science & Technology, Xi'an 710021, People's Republic of China

Received 28 May 2007; accepted 8 February 2008

DOI 10.1002/app.28220

Published online 9 May 2008 in Wiley InterScience (www.interscience.wiley.com).

ABSTRACT: Crosslinked starch microspheres (CSMs) were prepared in an inverse suspension system. Scanning electron microscopy observation indicated that the CSMs were uniform in granularity with a smooth spherical particulate surface. The particle size analysis revealed that the average diameter was 18.2 μm and that 85.8% of the microspheres were of a diameter below 30 μm . The structural characteristics of the carbonyl group and the second acrylamide by Fourier transform infrared spectroscopy of the CSMs showed that the soluble starch obviously cross-linked with *N,N'*-methylene bisacrylamide. The physical properties of the CSMs were analyzed by way of X-ray diffraction, differential scanning calorimetry, and thermogra-

vimetric analysis. The results show that the crosslinking resulted in an increase in thermal stability and a decrease in crystallinity of the CSMs compared with soluble starch. The adsorption capacity of the CSMs increased with increasing concentration of methylene blue. The lower temperature was in favor of the adsorption capacity of the CSMs. The adsorption mode of methylene blue by the CSMs agreed more with the Langmuir isothermal equation. © 2008 Wiley Periodicals, Inc. *J Appl Polym Sci* 109: 2571–2575, 2008

Key words: adsorption; structure; synthesis; thermal properties

INTRODUCTION

Starch microspheres are artificial derivatives of natural starch. They are capable of targeting drug delivery and biocompatibility. They are not only biodegradable but show a high degree of swelling in aqueous media. Therefore, they can form a gel-like bioadhesive system and can automatically adjust their shapes according to changes in the microenvironment in organisms.^{1,2} There exist many active sites and groups in the starch molecules that can be modified. The physical and chemical properties of starch microspheres may be controlled and adjusted by regulation of the synthesis techniques or by modification of the surface of the groups. According to the interaction mechanism, the drug-carrying function of starch microspheres are divided into three types: adsorption type, chemical coupling type, and embedding type, of which the adsorption method is the optimal mode and is suitable to most drugs. The drug-carrying capability of starch microspheres can

last for a comparatively long time before the degradation of its framework. So prolonging the drug-release time can improve the curative effect. As a carrier for targeting drug delivery, the application of starch microspheres is most promising for the nasal delivery system, artery embolization therapy, and pharmacokinetics.^{3–5}

Starch microspheres are often created by the crosslinking reaction of starch or modified products of starch with POCl_3 , $\text{Na}_3\text{P}_3\text{O}_9$, epichlorohydrin, or terephthalyl chloride.^{6–8} However, the products synthesized by the reported methods are not very ideal for carrying and releasing drugs. *N,N'*-methylene bisacrylamide (MBAA) can be used as a crosslinker to participate in the synthesis reaction of starch microspheres in the form of short-chain radicals. This synthesis is based on the reaction mechanism of free radicals and is different from the reported methods.⁹

In this study, a new type of crosslinked starch microsphere (CSM) was synthesized in an inverse suspension system with soluble starch (ST) as a raw material, MBAA as a crosslinker, and $\text{K}_2\text{S}_2\text{O}_8$ – Na_2SO_3 as an initiator. The microsphere size and size distribution of the CSM were determined. The structure and the properties of the CSM were studied with scanning electron microscopy, Fourier transform infrared (FTIR) spectroscopy, X-ray

Correspondence to: Z.-J. Li (lizhj@sust.edu.cn).

Contract grant sponsor: National Natural Science Foundation of China; contract grant number: 50573046.

diffraction (XRD), differential scanning calorimetry (DSC), and thermogravimetric analysis (TGA).

EXPERIMENTAL

Materials

The materials included ST [analytical reagent (AR), Shenyang Beifeng Chemical Reagent Factory (Shenyang, China)], cyclohexane, chloroform, sodium hydroxide, $K_2S_2O_8$, Na_2SO_3 , ethyl acetate, acetone, anhydrous ethanol, methylene blue (AR, Tianjin Damao Chemical Reagent Factory (Tianjin, China)), Span60 (AR, Shanghai Yuanji Chemical, Ltd. (Shenyang, China)), Tween60 (AR, Beijing Qingshengda Chemical Co., Ltd. (Beijing, China)), and MBAA (AR, Beijing Hengyezhongyuan Chemical Co., Ltd. (Beijing, China)). The water used was distilled water.

Synthesis of the CSM

The CSMs were prepared in a three-necked flask with an electric stirrer, a digital temperature-indicating/controlling instrument, and a reflux condenser. The temperature of the flask was maintained with a thermostatic water bath. ST (2 g) was dissolved in 20 mL of distilled water and stirred. The pH value was adjusted to 8 by sodium hydroxide. The mixture was heated with a water bath while it was stirred. The temperature was kept at 80°C for 30 min to ensure that the starch was dissolved completely. Then, the temperature was decreased to 50°C. Cyclohexane (80 mL) and chloroform (20 mL) were placed in a three-necked flask and heated with a water bath to 50°C under conditions of reflux. Span60-Tween60 (1 g) as an emulsifier was added. The water phase was added to the oil phase while the mixture was stirred. The emulsification effect was checked after 30 min. After the oxygen was ejected completely from the three-necked flask by a nitrogen flow, 0.2 g of MBAA, 0.04 g of $K_2S_2O_8$, and a proper amount of Na_2SO_3 were added. The crosslinking reaction was carried out for 2 h at a temperature of 50°C. The reaction solution was removed and separated by centrifugation. The underlayer crosslinked polymers were subsequently washed with ethyl acetate, acetone, and anhydrous ethanol. Then, they were dried, and a white or pale yellow CSM powder was obtained.

Characterization of CSM

The morphology of CSM was evaluated through SEM (JSM-6460 SEM, Jeol (Tokyo, Japan)) observation. The microsphere size and the size distribution were determined with a particle size analyzer (SKC-2000, Japan Seishin). The structure character was analyzed by FTIR spectroscopy (VECTOR-22, Bruker

(Ettlingen, Germany)) with highly pure potassium bromide tableting. The physical properties were determined with XRD (D/max 2000PC, Rigaku Corp. (Tokyo, Japan) with $2\theta = 10\text{--}70^\circ$) and a thermoanalyzer system (Q1000DSC+LNCS+FACS Q600SDT, TA Instruments (New Castle, Delaware, USA) with N_2 ambience and a heating rate of 20.00°C/min).

Determination of the adsorption isotherm

The adsorption experiment was carried out in 250-mL Erlenmeyer flasks equipped with stoppers, in which 0.1000 g of the CSMs and different concentrations of methylene blue were added. The Erlenmeyer flasks were vibrated at a speed of 100 rpm for 12 h. The temperature was controlled at 298, 308, and 318 K. The absorbency of the solutions was determined with a UV-visible spectrophotometer (UV-265FW, Shimadzu Corp. (Kyoto, Japan)) at $\lambda = 655$ nm (operating curve $A = 58.14c + 10.28$, $R^2 = 0.9981$). The equilibrium adsorption capacity (Q_e ; mmol/g) was calculated according to eq. (1):

$$Q_e = \frac{V(c_0 - c_e)}{m} \quad (1)$$

A : is the solution absorbency; C : is the solution concentration, mmol/L, where c_0 is the initial concentration (mmol/L), c_e is the equilibrium concentration (mmol/L), V is the solution volume (L), and m is the mass of the CSMs (g).^{10,11}

RESULTS AND DISCUSSION

Morphological and dimensional analysis of the CSMs

As shown in Figure 1, the synthesized CSM was a spherical particulate with a smooth surface, which implied a homogeneous and dense structure. These microspheres were analyzed with a particle size analyzer. The results show that 85.8% of the microspheres were below 30 μm and the average diameter was about 18.2 μm (see Fig. 2).

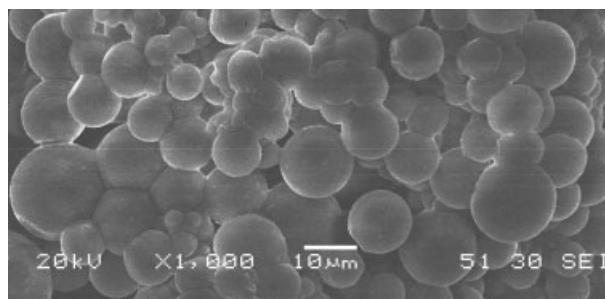


Figure 1 SEM micrograph of the starch microspheres.

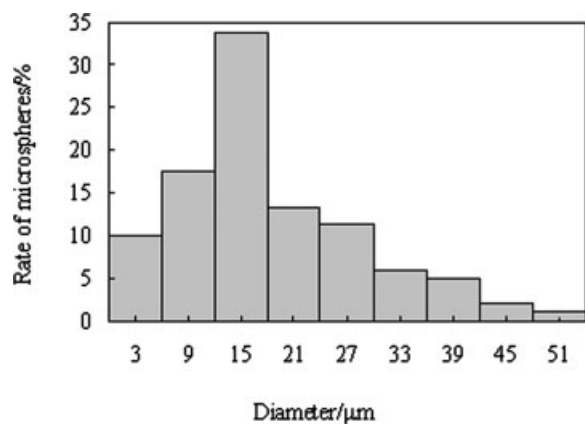


Figure 2 Size distribution of the starch microspheres.

Structure analysis of the CSMs

Figure 3 shows the comparative FTIR spectrograms of the CSM and ST. Characteristic peaks appeared at 3445 cm^{-1} (CSM) and 3443 cm^{-1} (ST). This indicated that the hydroxyl group existed before and after the crosslinking reaction, but the production of the starch microspheres resulted in the weakening of the association between hydrogen bonds. Consequently, the absorption peak of the CSM became lankier and shifted slightly to the high-frequency region. The absorption peaks at 2928 cm^{-1} in the two curves belonged to the stretching vibration of the C—H bonds of glucose units, whereas the bending vibration of these bonds was noticed at 1384 cm^{-1} . The absorption peaks at 1154 cm^{-1} (CSM) and 1162 cm^{-1} (ST) corresponded to the C—C stretching vibration, and the peaks at 1109 cm^{-1} (CSM) and 1082 cm^{-1} (ST) were related to the C—O—C stretching vibration. The peaks at 1140 cm^{-1} (CSM) and 1050 cm^{-1} (ST) corresponded to the C—OH stretching vibration of starch molecules. The presence of

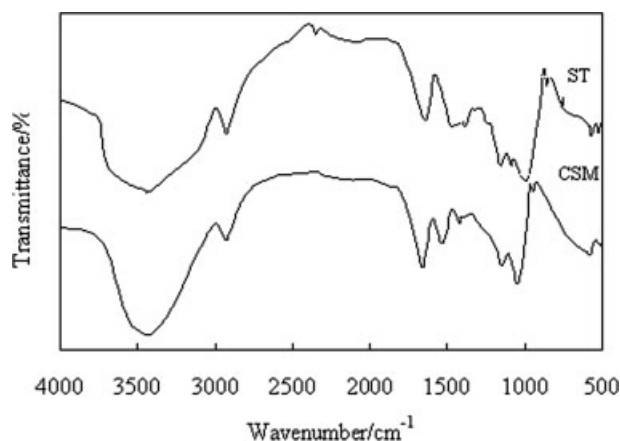


Figure 3 FTIR spectrograms of the ST and starch microspheres.

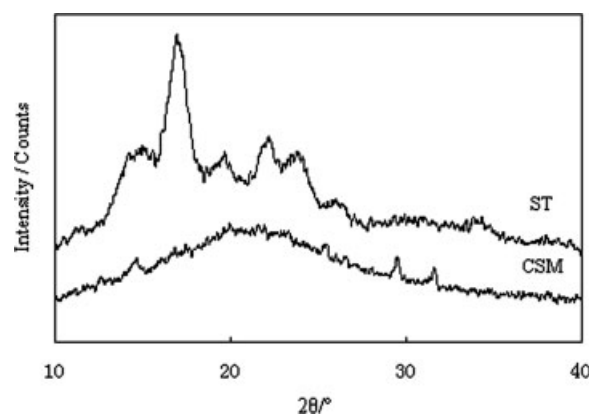


Figure 4 XRD patterns of the ST and starch microspheres.

these peaks verified that the basic structural units of starch were not markedly changed by the formation of crosslinking bonds in the structure of the CSM. In the FTIR curve of the CSM, the absorption peak presenting at 1652 cm^{-1} belonged to the stretching vibration of carbonyl groups, and the absorption peak at 1538 cm^{-1} was the remarkable characteristic of the second acrylamide. Thus, we deduced that apparently, a crosslinking reaction took place between ST and MBAA.

Physical properties of the CSM

Analysis of XRD

Figure 4 displays the analysis results of XRD of the ST and CSM. The sharp peaks of diffraction at $2\theta = 16.8, 20, 22.4, \text{ and } 23.6^\circ$ occurred in the spectrogram of ST, and the measured degree of crystallinity was about 33%. At $16.8, 22.4, \text{ and } 23.6^\circ$, the peaks of diffraction disappeared completely, and the relative intensity of the diffraction peak of the CSM at 20° obviously decreased. Meanwhile, its amorphous area got correspondingly wider, and the peaks of diffraction at $14.6, 29.3, \text{ and } 31.6^\circ$ appeared simultaneously weaker. The degree of measured crystallinity was about 6.4% in the spectrogram of the CSM. The variations were attributed to the crosslinking reactions, which restricted the activity of the starch molecules, destroyed the regularity of the starch molecule, and weakened the intermolecular forces of the starch molecular chains and the hydrogen bond. Therefore, the crystallization capacity was reduced.¹²

Analysis of DSC

As shown in Figure 5, there were two big endothermic peaks and one obvious weak peak of exothermic decomposition in each curve of heat flow in the DSC diagrams of the ST and CSM. The endothermic peaks at $105 \text{ and } 101^\circ\text{C}$ were caused by heat absorp-

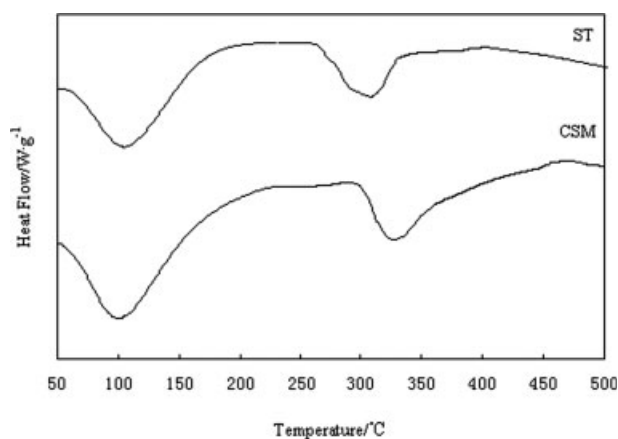


Figure 5 DSC curves of the ST and starch microspheres.

tion and water loss. The initial temperature of water loss of the CSM was lower than that of the ST, which indicated that the crosslinking resulted in an increase in the porosity of the CSM so as to make more moisture be absorbed. The endothermic peaks at 308 and 328°C had a connection with the fission of macromolecule chains when huge amounts of heat were absorbed by the starch molecule and CSM. The peaks of exothermic decomposition of the ST and CSM appeared at 403 and 466°C, respectively. The previous data demonstrate that the crosslinking reaction resulted in an increase in the thermal stability of the CSM. The glucose units were decomposed at above the temperatures of the peaks of thermal decomposition, and the samples started to carbonize.¹³

Analysis of TGA

The TGA curves of the ST and CSM are shown in Figure 6. The degradation procedure of each sample

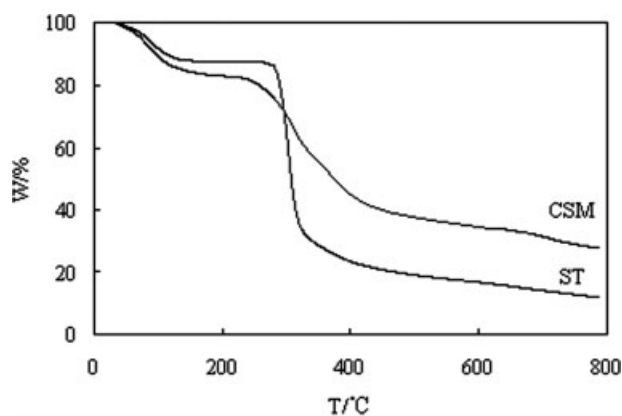


Figure 6 TGA curves of the ST and starch microspheres. $W = m_t/m_0$ (m_0 is the initial sample quality, m_t is the remaining sample quality at the temperature T), T is the temperature, °C.

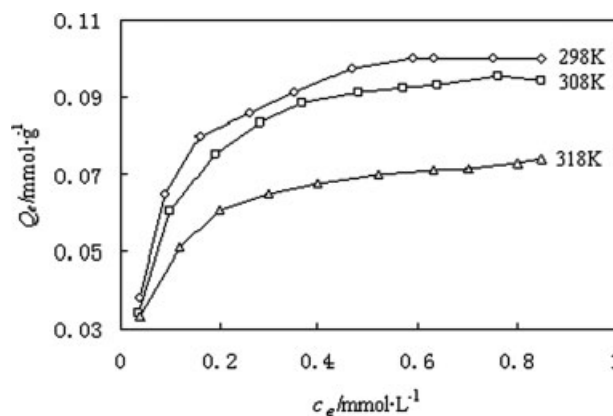


Figure 7 Adsorption isotherm of methylene blue by the CSMs.

could be divided into two stages according to Figure 6. The first stage ranged from room temperature to 200°C, in which the rates of weight loss of the ST and CSM were about 12 and 17%, respectively. The starting point of the first stage of the CSM appeared at a lower temperature in comparison with ST. The rate of weight loss in the first stage was mainly caused by water loss in both the ST and CSM. Furthermore, the drop in the temperature of water loss and the increase in the moisture content were related to the increase in pore spaces resulting from crosslinking in the structure of the CSM and the increased rate of free moisture. It also indicated, to a certain extent, the change in the strength of the water molecules combining with the surface groups of the CSM. The degradation process in the second stage corresponded to the decomposition of glucose units and the rupture of the main chains of starch molecules and crosslinking bonds. Within a certain range of temperature, the rate of weight loss of ST increased rapidly, whereas that of the CSM increased more slowly. Thus, we affirmed that these changes rested with the function of balling crosslinking and the decrease in the crystallinity of the CSM.

Analysis of adsorption capacity of the CSM

Isothermal adsorption curve of the CSM

Figure 7 shows the isothermal adsorption curves of methylene blue by the CSM at 298, 308, and 318 K. The experimental results show that the adsorption capacity of the CSM increased with increasing concentration of methylene blue. Also, the lower temperature was in favor of the adsorption capacity of the CSM at the same concentration. This was mainly due to the fact that the molecular energy of methylene blue decreased with the drop in temperature such that it was more easily adsorbed.

TABLE I
Langmuir and Freundlich Isotherm Constants

| Temperature (K) | Langmuir model | | | Freundlich model | | |
|-----------------|----------------|--------------|--------|------------------|-------|--------|
| | Q_0 (mmol/g) | b (L/mmol) | R^2 | K_F | n | R^2 |
| 298 | 0.1064 | 18.73 | 0.9978 | 0.1159 | 3.686 | 0.9179 |
| 308 | 0.1042 | 13.89 | 0.9997 | 0.1109 | 3.312 | 0.9067 |
| 318 | 0.0768 | 19.07 | 0.9964 | 0.0808 | 4.183 | 0.9269 |

Analysis of adsorption equilibrium

The isothermal adsorption curve can be approximately expressed by a mathematical equation with an adsorption model. The correlation between c_e of the solute obtained from the experiments and Q_e of the sorbent of the unit mass accords with a certain mathematical formula, according to which the unmeasured saturated adsorption capacity (Q_0 ; mmol/g) is calculated. Actually, the Langmuir equation and the Freundlich equation are the most commonly used calculation formulas for processing the experimental data of liquid-phase adsorption provided that the sorption of the solvent is ignored. The verification method of the experimental data to the Langmuir model is to substitute the experimental data into eq. (2) and validate their linear relationship:

$$\frac{1}{Q_e} = \frac{1}{Q_0} + \frac{1}{bQ_0} \times \frac{1}{c_e} \quad (2)$$

where Q_e is the equilibrium adsorption capacity of methylene blue by CSM (mmol/g), b is the adsorption equilibrium constant, and c_e is the equilibrium concentration of methylene blue in the solution (mmol/L).

In the same way, the confirmation of the experimental data to the Freundlich model is to substitute the experimental data into eq. (3) and validate their linear relationship:

$$\ln Q_e = \ln K_F + \frac{1}{n} \times \ln c_e \quad (3)$$

where Q_e is the equilibrium adsorption capacity of methylene blue by CSM (mmol/g), c_e is the equilibrium concentration of methylene blue in the solution (mmol/L), and K_F and $1/n$ are the adsorption constants.

The experimental data were processed with regression analysis according to eqs. (2) and (3), and the results are listed in Table I. As shown in Table I, the adsorption model of methylene blue by CSM agreed more with the Langmuir isothermal equation.

CONCLUSIONS

Homogeneous and dense CSMs with acylamino were prepared through chemical crosslinking reactions in an inverse suspension system. The average diameter of the microspheres was around 18.2 μm . Compared with ST, the crystallinity of the CSMs decreased and the thermal stability increased because of crosslinking. The crosslinking restricted the activity of the starch molecules, destroyed the regularity of the starch molecules, and weakened the intermolecular force of the starch molecular chains and the hydrogen bond. The adsorption mode of methylene blue by the CSMs agreed more with the Langmuir isothermal equation. CSMs are expected to be used for drug loading because of their outstanding adsorption capacity.

The authors thank Zhen-Hai Shi for his experimental assistance.

References

- Illum, L.; Jorgensen, H.; Bisgaard, H.; Krogsgaard, O.; Rossing, N. *Int J Pharm* 1987, 39, 189.
- Illum, L.; Fisher, A. N.; Jabbal-Gill, I.; Davis, S. S. *Int J Pharm* 2001, 222, 109.
- Björk, E.; Edman, P. *Int J Pharm* 1990, 62, 187.
- Shiba, H.; Okamoto, T.; Futagawa, Y.; Misawa, T.; Yanaga, K.; Ohashi, T.; Eto, Y. *J Surg Res* 2006, 133, 193.
- Suzuki, M.; Nagata, K.; Masunaga, S.; Kinashi, Y.; Sakurai, Y.; Maruhashi, A.; Ono, K. *Appl Radiat Isot* 2004, 61, 933.
- Yu, J. G.; Tian, R. C.; Liu, Y. Q. *Chem Res Chin Univ* 1994, 15, 616.
- Fundueanu, G.; Constantin, M.; Dalpiaz, A.; Bortolotti, F.; Cortesi, R.; Ascenzi, P.; Menegatti, E. *Biomaterials* 2004, 25, 159.
- Mao, S. R.; Chen, J. M.; Wei, Z. P.; Liu, H.; Bi, D. Z. *Int J Pharm* 2004, 272, 37.
- Zhao, X. F.; Li, Z. J.; Wang, L.; Xiao, H. J.; Liu, J. G.; Cai, J. R. *Chem Eng* 2007, 35, 66.
- An, J. H.; Dultz, S. *Appl Clay Sci* 2007, 36, 256.
- Coelho, T. C.; Laus, R.; Mangrich, A. S.; Fávère, V. T.; Laranjeira, M. C. M. *React Funct Polym* 2007, 67, 468.
- Cao, Y. X.; Zhang, C.; Ping, Q. N. *Polym Mater Sci Eng* 2005, 21, 236.
- Zhao, Y. Z.; Bai, F.; Huang, W. Q. *Acta Polym Sinica* 2004, 48, 410.